RSC Advances

PAPER

View Article Online
View Journal | View Issue

Cite this: *RSC Adv.*, 2025, **15**, 15108

Iodine-mediated synthesis of indolyl-1,3,4-thiadiazole amine derivatives and their DFT analysis†

Vartika Vaishya,[a] Manish K. Mehra,‡[b] S. K. Pandey[c] and Meenakshi Pilania *[a]

Received 22nd March 2025
Accepted 21st April 2025

DOI: 10.1039/d5ra02026c

rsc.li/rsc-advances

An effective iodine-mediated one-pot three-component strategy for the construction of indolyl-1,3,4-thiadiazole amines has been described. The method involved the reaction of tosylhydrazine with indole-3-carboxaldehyde and ammonium thiocyanate as a non-toxic source of sulphur under metal-free conditions. The developed protocol included readily available substrates, shorter reaction time, use of low-toxic thiocyanate, and benzylation with a broad substrate scope, making it a viable approach for multiple applications. Furthermore, DFT analysis was conducted using the Gaussian 09 package.

1. Introduction

Due to their peculiar scaffold of the indole nucleus, many natural and synthetic indolyl heterocycles have already been investigated for their biological roles.[1–7] Indolylazoles and indolylthiazoles (camalexin[8] and the naturally occurring BE 10988 (ref. 9)) are well known for their cytotoxic properties against human cancer cell lines.[10–13] Interestingly, other biologically active indolyl derivatives include bis(indole) alkaloids,[14–16] nortopsentins,[17] chondramide A (an antiviral agent),[18,19] α-cyclopiazonic acid (a muscle relaxant),[20] brassinin and cyclobrassinin (antimicrobial),[21,22] caulilexins A (an antifungal agent),[23] and compounds involved in the treatment of type 2 diabetes mellitus.[24] (Fig. 1). Similarly, 1,3,4-thiadiazole amines belong to the class that displays a wide range of biological properties,[25–31] such as antitubercular,[32] antimicrobial,[33,34] antiviral,[35] cancer cell apoptosis,[36] among others (Fig. 1). In view of their immense biological significance, many synthetic approaches for the construction of indolyl-1,3,4-thiadiazole amines have been developed.[37,38] For instance, Kumar and co-workers described the synthesis of indolyl-1,3,4-thiadiazole amines involving a multi-step approach, starting from indole-3-carboxylic acids as the initial substrates (Scheme 1a).[39] The typical strategy for the preparation of indolyl-1,3,4-thiadiazole amines primarily involves the heating of *N*-aminothiourea and indole-3-carboxylic acid in $POCl_3$, followed by hydrolysis in water (Scheme 1b).[40] As depicted in Scheme 1c, the reaction of thiosemicarbazide with indole-3-carboxaldehydes in methanol under reflux affords indole-3-thiosemicarbazones, which, upon heating at 90 °C in a $FeCl_3$ solution, undergo cyclization to produce indolyl-1,3,4-thiadiazole amines.[41]

It is noteworthy that these procedures typically involve multi-step synthetic approaches for the construction of indolyl-1,3,4-thiadiazole amines. As shown in Scheme 1d, the indolyl-1,3,4-thiadiazole amines have been synthesized by heating indole-3-carbonitriles with thiosemicarbazide under acidic (TFA) conditions.[42] However, this approach (Scheme 1d) requires indole-3-carbonitriles as substrates, which are generally expensive or require an additional synthetic step for their

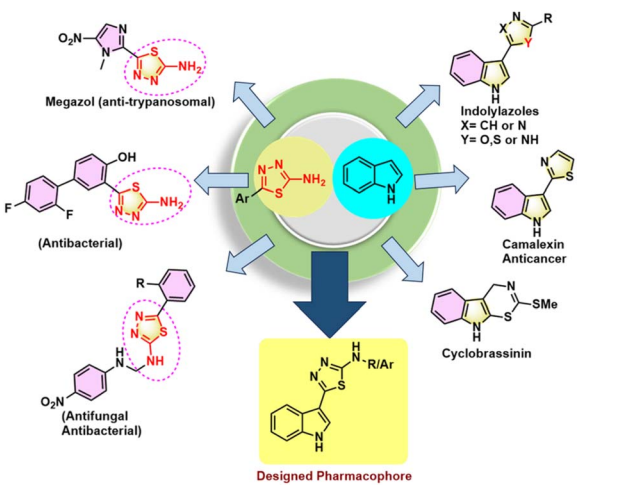

Fig. 1 Medicinal applications of indolylthiazoles and aminothiadizoles.

[a]*Department of Chemistry, School of Physical and Biological Sciences, Manipal University Jaipur, VPO- Dehmi-Kalan, Off Jaipur-Ajmer Express Way, Jaipur, Rajasthan, 303007, India. E-mail: meenakshi.pilania@jaipur.manipal.edu; meenakshi.pilania1987@gmail.com*

[b]*Department of Chemistry, Gachon University, 1342 Seongnamdaero, Seongnam, Gyeonggi, 13120, Republic of Korea*

[c]*Department of Chemistry, Maulana Azad National Institute of Technology Bhopal, Bhopal, Madhya Pradesh, 462003, India*

† Electronic supplementary information (ESI) available. See DOI: https://doi.org/10.1039/d5ra02026c

‡ The Wistar Institute, Philadelphia, PA, 19104, USA.

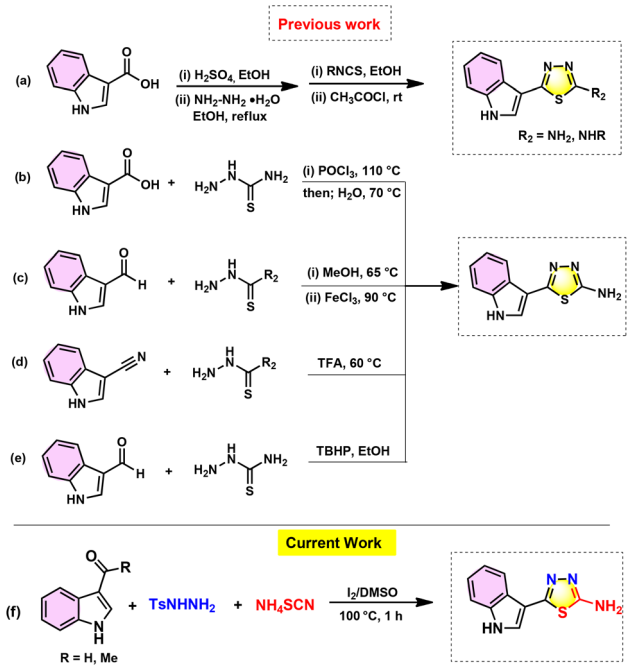

Scheme 1 Synthetic routes for Indolyl-1,3,4-thiazole amine.

preparation. Likewise, Perike *et al.* recently disclosed that when thiosemicarbazide reacts with indole-3-carboxaldehyde in *tert*-butyl hydroperoxide (TBHP), it affords indolyl-1,3,4-thiadiazole amine (Scheme 1e).[43] Although the Perike group developed this one-step protocol (Scheme 1e), the preparation of indolyl-1,3,4-thiadiazole amine was limited to a single example. Despite numerous efforts presented thus far, the existing protocols to prepare indolyl-1,3,4-thiadiazole amines involve pre-functionalized starting materials, harsh or environmentally unfavourable reaction conditions, moisture-sensitive reagents, and expensive or lengthy syntheses.

Hence, developing operationally simple and mild reaction conditions is highly desirable. In the recent past, *N*-tosylhydrazones have gained considerable attention owing to their high stability and versatility for a range of synthetic transformations, including reductions, carbenoid chemistry, cross-coupling reactions under metal-catalysed[44] or metal-free reaction conditions, as well as functionalization and the preparation of heterocycles.[45–47] *N*-Tosylhydrazone, a particular carbene species, has been used to synthesize numerous biologically active motifs with a wide scope of applications,[48] such as thiadiazole derivatives,[49–52] tetrazole derivatives,[53] pyrazole derivatives,[54] and oxazine derivatives.[55] Recently, the combination of I_2 and DMSO has become a popular and environmentally benign oxidative system for organic synthesis.[56–59] Owing to its easy availability and high reactivity, iodine is frequently used in the synthesis of 1,3,4 thiadiazole and 1,3,4-oxadiazoles.[60–69] Yu and colleagues developed a synthetic protocol leading to 2-amino-1,3,4-thiadiazole and 2-amino-1,3,4-oxadiazole from the reaction of semicarbazide/thiosemicarbazide with aldehyde derivatives using iodine.[62]

Zhu and colleagues revealed an efficient method for synthesizing 2-amino-1,3,4-thiadiazole using *N*-tosylhydrazones, potassium thiocyanate (KSCN) and iodine.[70] However, this aforementioned protocol was limited to benzaldehyde analogues.[70,71] To overcome the limitations of existing methods, we aimed to develop a direct, efficient, eco-friendly, and cost-effective protocol to synthesize indolyl-1,3,4-thiadiazole amine.

Herein, we report a direct single-step synthesis of indolyl-1,3,4-thiadiazole amine from the reaction of readily accessible indole-3-carboxaldehyde and $TsNHNH_2$ using ammonium thiocyanate (NH_4SCN) as a sulphur source in the presence of I_2 (iodine)/DMSO as an oxidative system (Scheme 1f).

2. Results and discussion

2.1 Chemistry

Initially, we chose the reaction of indole-3-carboxaldehyde (**1a**, 1.38 mmol) and tosylhydrazine (1.38 mmol) with KSCN (2.76 mmol) as the model reactions to optimize the reaction conditions. All the findings are summarized in Table 1. The treatment of **1a** with tosylhydrazine using KSCN in the presence of molecular iodine (I_2; 1.5 equiv.) in DMSO at 100 °C yielded the desired product 5-(1*H*-indol-3-yl)-1,3,4-thiadiazol-2-amine (**3a**) in 70% yield after 5 h (Table 1, entry 1). We then endeavored to manipulate the reaction condition by adding additives such as $K_2S_2O_8$, Na_2CO_3, K_2CO_3 and Cs_2CO_3 along with iodine, which showed slightly higher efficiency in the formation of desired product **3a** in 20–55% yields (Table 1, entry 2–5). It was observed that the use of copper catalysts, such as CuI and $CuCl_2$, as additives was futile, and the formation of desired product **3a** was not observed (Table 1, entry 6–7). Thus, these findings

Table 1 Optimization of reaction conditions for **3a** [a]

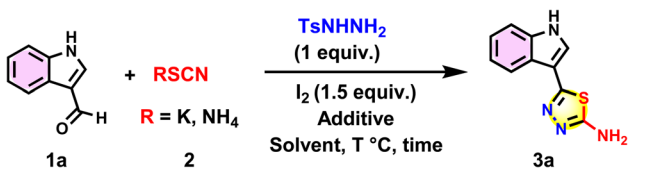

Entry	2	Solvent	Additive	Time (h)	*T* (°C)	Yield[b] (%)
1	KSCN	DMSO	—	5	100	70
2	KSCN	DMSO	$K_2S_2O_8$	2.5	100	20
3	KSCN	DMSO	Na_2CO_3	2.5	100	55
4	KSCN	DMSO	K_2CO_3	2.5	100	32
5	KSCN	DMSO	Cs_2CO_3	2.5	100	30
6	KSCN	DMSO	CuI	2.5	100	ND[d]
7	KSCN	DMSO	$CuCl_2$	2.5	100	ND[d]
8	NH_4SCN	DMSO	—	1	100	88
9	NH_4SCN	DMSO	—	1	100	72[c]
10	NH_4SCN	EtOH	—	18	78	ND[d]
11	NH_4SCN	DMF	—	1	50	50
12	NH_4SCN	Toluene	—	2.5	100	Trace
13	KSCN	DCE	—	2.5	100	Trace

[a] Reaction conditions: **1a** (1.38 mmol), **2** (2.76 mmol, 2 equiv.), *p*-toluenesulfonyl hydrazide (1.38 mmol, 1 equiv.), iodine (2.07 mmol, 1.5 equiv.), and solvent (2.0 mL) in a sealed tube for 1 h at 100 °C. [b] Isolated yields. [c] 1.5 equiv. of NH_4SCN was used. [d] ND = not determined.

(Table 1, entry 2–7) imply that additives negatively impact the outcome of the reaction. Remarkably, the productivity of the reaction was increased to provide an 88% yield of **3a** after 1 h when KSCN was substituted with NH_4SCN without the addition of any additives (Table 1, entry 8). Next, decreasing the equivalent of NH_4SCN from 2.0 to 1.5 equivalents resulted in a relatively low yield of **3a** (Table 1, entry 9). Later, the screening of various solvents such as EtOH, DMF, toluene and DCE (1,2-dichloroethane) was ineffective in ameliorating the yield of **3a** (Table 1, entry 10–13).

Finally, we uncovered that the ideal conditions for the reaction of **1a** to produce an acceptable yield of **3a** in 1 h were the use of iodine (1.5 equiv.), *p*-toluenesulfonyl hydrazide (1 equiv.), and NH_4SCN (2 equiv.) in DMSO at 100 °C.

The reaction of **1** with electron-rich (methoxy), halo (bromo, chloro and fluoro), and electron-deficient (nitro) substitutions was used to investigate the generality of the optimized methodology (Scheme 2). Reaction with electron-neutral (**1a**), electron-rich (OMe; **1b**), halogen (Br, Cl; **1c**, **1d**) bearing at the C5-position and halogen (F; **1e**) at the C4-position of indole-3-carboxaldehydes produced the corresponding 5-(1*H*-indol-3-yl)-1,3,4-thiadiazol-2-amines (**3a–e**) in excellent yields (80–91%). Nonetheless, indole-3-carboxaldehyde **1f**, having an electron-deficient nitro group, exhibited diminished reactivity, resulting in the formation of **3f** with a slightly reduced yield of 65% (Scheme 2).

To demonstrate the synthetic usefulness of this developed protocol, we targeted the gram-scale synthesis of 5-(1*H*-indol-3-yl)-1,3,4-thiadiazol-2-amine **3a** (Scheme 2). Fortunately, under standard conditions, the reaction of 1.0 g **1a** (6.89 mmol) under optimized conditions gave 1.28 g of desired product **3a** in an 86% yield.

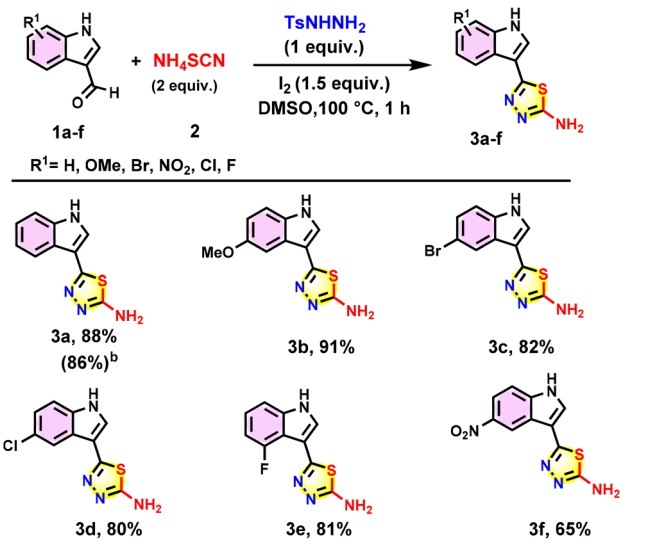

Scheme 2 Synthesis of 5-(1*H*-indol-3-yl)-1,3,4-thiadiazol-2-amines **3a–f**. [a]Reaction conditions: **1a–f** (1.38 mmol), **2** (2.76 mmol, 2 equiv.), *p*-toluenesulfonyl hydrazide (1.38 mmol, 1 equiv.), iodine (2.07 mmol, 1.5 equiv.), and DMSO (2.0 mL) in a sealed tube for 1 h at 100 °C. [b]Reaction was performed on a 1 g scale.

Next, we focused on exploring the utilization of 3-acetylindole instead of 3-formylindole (**1a**). Unfortunately, when we utilized 3-acetylindole under the developed conditions, the desired product was not detected. Therefore, we slightly modified our strategy. First, we prepared the corresponding *N*-tosylhydrazone of 3-acetylindole (**1g**), as described in the literature.[72] Further, the investigation concluded that the use of ethanol as a solvent and the addition of 1 equiv. of $K_2S_2O_8$ are required to obtain the expected 2-(1*H*-indol-3-yl)-1,2,3-thiadiazole (**3g**) in 82% yield (Scheme 3).

We further focused on the exploration of the *N*-alkylation of 5-(1*H*-indol-3-yl)-1,3,4-thiadiazol-2-amine **3a** owing to the significance of 2-*N*-(alkylamino)thiadiazoles, the distinct reaction properties of tosylhydrazones, and the emergence of difficult C–N bond formation approaches. In this regard, the reaction was optimized meticulously by changing various factors, and the results are presented in Table 2.

The first attempt involved a reaction between **3a** and **4a** in toluene at 100 °C for 2 h using 10 mol% CuI and Na_2CO_3 as a base. Unfortunately, only trace amounts of the desired product (**5a**) were observed (Table 2, entry 1). Next, the changing base from Na_2CO_3 to Cs_2CO_3 and LiO*t*Bu resulted in the formation of **5a** in 30% and 70%, respectively (Table 2, entry 2–

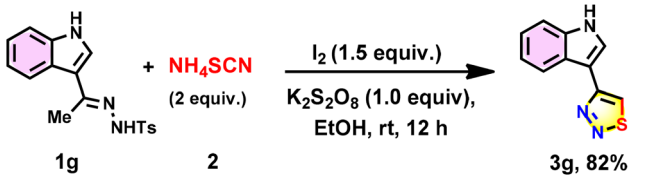

Scheme 3 Synthesis of 2-(1*H*-indol-3-yl)-1,2,3-thiadiazole **3g**. [a]Reaction Conditions: **1g** (0.61 mmol), **2** (1.22 mmol, 2 equiv.), iodine (0.92 mmol, 1.5 equiv.), $K_2S_2O_8$ (0.61 mmol, 1 equiv.), and EtOH (2.0 mL) for 12 h at rt.

Table 2 Optimization of reaction conditions for the *N*-alkylation of 3a [a,b]

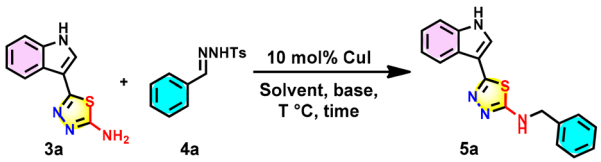

Entry	Base	Solvent	*T* (°C)	Time (h)	Yield (%)
1	Na_2CO_3	Toluene	100	2	Trace
2	Cs_2CO_3	Toluene	100	3	30
3	Li-*t*-OBu	Toluene	100	3	70
4	Li-*t*-OBu	Toluene	110	2.5	80
5	Li-*t*-OBu	Toluene	120	2.5	78
6	Li-*t*-OBu	Xylene	110	2.5	75
7	Li-*t*-OBu	DMSO	110	3	ND[c]

[a] Reaction conditions: **3a** (0.46 mmol, 1 equiv.), **4a** (0.46 mmol, 1 equiv.), CuI (0.046 mmol, 0.1 equiv.), LiOtBu (0.69 mmol, 1.5 equiv.), and toluene (1.5 mL) in a sealed tube for 2.5 h at 110 °C. [b] Isolated yields. [c] ND = not determined.

3). Notably, a higher product yield (**5a**, 80%) was observed when the reaction temperature was increased from 100 °C to 110 °C (Table 2, entry 4). However, when the temperature of the reaction mixture was further increased to 120 °C, the yield of **5a** was reduced to 78% (Table 2, entry 5). The use of another non-polar solvent, xylene, resulted in a relatively lower product yield (75%) of **5a** (Table 2, entry 6). It was observed that when DMSO, a polar solvent, was used for the reaction, the expected product **5a** was not detected, indicating the toxic behaviour of polar solvents on the reaction outcome (Table 2, entry 7). Thus, 10 mol% of CuI with 1.5 equiv. of LiO*t*Bu in toluene at 110 °C was the optimal condition for the benzylation of **3a** using **4a**.

Upon establishing suitable reaction conditions (Table 2, entry 4), we assessed the generality of the *N*-benzylation reaction by utilizing a series of tosylhydrazones **4a–l**. As shown in Scheme 4, tosylhydrazone with electron neutral (**4a**) and halogen (Br; **4b** and F; **4c**) substituents on the aromatic ring produced products in good yields (**5a–c**). Tosylhydrazones with electron-donating substituents, such as -NMe_2 (**4d**), -OMe (**4e** and **4f**), and -OBn (**4g**), either at *meta*- or *para*-positions, slightly affected the product yield, giving corresponding **5d–g** in 38–62% yields. It is important to mention that the tosylhydrazone bearing a base-sensitive hydroxy group (**4h**) could deliver desired product **5h** in 30% yield. Remarkably, tosylhydrazone with electron-withdrawing substituents, such as nitro (**4i**) and cyano (**4j**), reacted efficiently to provide the expected products **5i** (80%) and **5j** (78%) in high yields. Notably, heterocyclic thiophene (**4k**) and benzophenone (**4l**) derived *N*-tosylhydrazone were also reacted. However, their products (**5k** and **5l**) were obtained in low yields (28–29%) (Scheme 4).

Scheme 5 shows a plausible mechanism for synthesizing indolyl-1,3,4-thiadiazole amine **3a** based on experimental observations and previous studies.[70] First, it is believed that **1a** reacts with *p*-toluenesulfonyl hydrazide to form *N*-tosylhydrazones **A** (Scheme 5). Tosylhydrazone **A** then probably gives iodonium ion **B** in the presence of molecular iodine (I_2). Subsequently, the attack of –the SCN ion results in the formation of intermediate **C**. This formed intermediate **C** is then converted to **D** by eliminating a hydrogen iodide (HI) molecule. Next, the intramolecular cyclization of **D** may provide intermediate **E**. Finally, intermediate **E** generates desired product **3a** by losing a molecule of *p*-methylbenzenesulfonic acid (TsOH) and capturing a proton *via* a hydrogen shift (Scheme 5).

Similarly, a plausible mechanism for the $I_2/K_2S_2O_8$-mediated reaction of *N*-tosylhydrazones **1g** and ammonium thiocyanate, leading to the synthesis of Indolyl-1,2,3-thiadiazole, is proposed in Scheme 6.[73] Initially, compound **1g** reacts with I_2 to form *α*-iodo substituted species **I**, generating I^-, which is reoxidized to I_2 by $K_2S_2O_8$. Intermediate **I** is then transformed into intermediate **II** by eliminating HI. Intermediate **II** reacts with NH_4SCN to produce intermediate **III**, which, upon tautomerization, produces intermediate **IV**. Intramolecular cyclization of **IV** was followed by the elimination of a cyanide ion in the presence of a base, yielding intermediate **V**. Finally, intermediate **V** releases TsH, resulting in the formation of the indolyl-1,2,3-thiadiazole product (**3g**). Notably, this reaction produced toxic CN^- ions and H^+ ions, which can release HCN gas as a byproduct (Scheme 6).

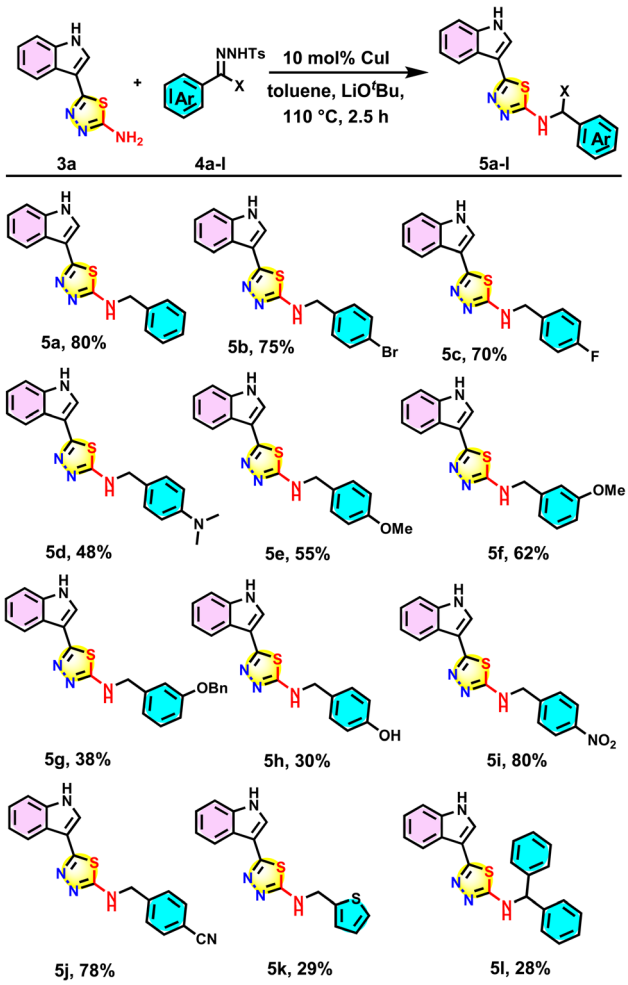

Scheme 4 CuI-catalyzed *N*-benzylation of **3a** using **4a–l**. [a]Reaction conditions: **3a** (0.46 mmol, 1 equiv.), **4a–l** (0.46 mmol, 1 equiv.), CuI (0.046 mmol, 0.1 equiv.), LiOtBu (0.69 mmol, 1.5 equiv.), and toluene (1.5 mL) in a sealed tube for 2.5 h at 110 °C.

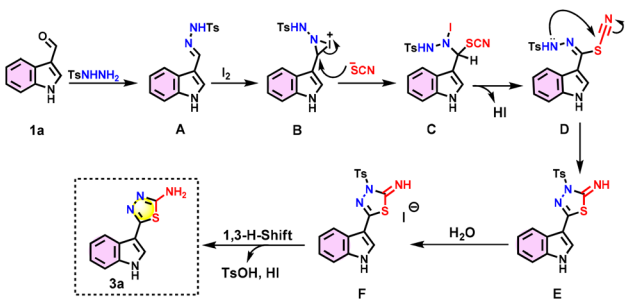

Scheme 5 Plausible mechanism for the synthesis of 5-(1*H*-indol-3-yl)-1,3,4-thiadiazol-2-amine (**3a**).

2.2 DFT analysis

Density functional theory (DFT)-based quantum calculations were employed to predict and investigate the structural/geometric properties, energetics, and electronic features relevant to biological activity. The B3LYP/6-31G+(d, p) level of the

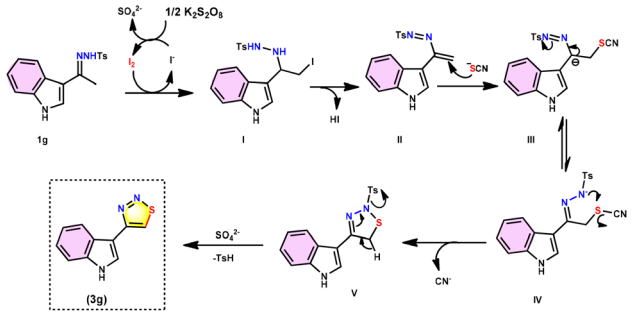

Scheme 6 Plausible mechanism for the synthesis of 4-(1*H*-indol-3-yl)-1,2,3-thiadiazole (**3g**).

DFT method is employed during the computational experiment. The *in silico* approach is deployed using electronic structure calculations with the Gaussian 09 package.[74] During optimization, the compounds were found to be at a minimum, and all frequencies were detected to be positive. Numerous studies have been conducted on the structural, stability, and electronic feature analyses of chemical species in composite materials.[75–77]

Molecular orbitals, such as the highest occupied molecular orbital (HOMO) and lowest unoccupied molecular orbital (LUMO), are obtained from frontier molecular orbitals (FMOs). The qualitative estimation of the HOMO–LUMO gap (HELG, denoted as E_{gap}) has important chemical implications. For any molecular system, such orbitals drop at the remotest edges of electrons, where the HOMO behaves like a Lewis base and consists of occupied (filled) orbitals with electrons exhibiting the highest occupied molecular orbital energy level, allowing them to easily donate electrons. However, another orbital named LUMO (*i.e.* immediate upper energy level of the HOMO) plays a role as a Lewis acid and has an unoccupied (vacant) orbital showing the lowest unoccupied molecular orbital energy level, which can easily accept the electrons from the HOMO. A crucial metric is that electron mobility can be determined from the HOMO to the LUMO. In general, a large HLEG value signifies a chemical species with good thermodynamic stability (chemically less reactive), while a small HLEG value indicates an easier electronic transition along with a chemically more reactive compound. The energetic contribution, especially the HLEG value (E_{gap}), is very important for the stability of any species. The energies of the HOMO (E_{HOMO}) and LUMO (E_{LUMO}) and their energy difference (E_{gap}) are shown in Fig. 2. Usually, a higher electronegativity of an atom or a group of atoms increases the acidic nature and the expected trend among the –OCH_3, -Br, and –NO_2 functional groups chosen in this study. The electronegativity order is –NO_2 > –OCH_3 (where Me → CH_3) > -Br, which appears to show a similar pattern for the acidity. However, considering the I-effect of the substituents reported by Robert Taft in 1958, the electron acceptors (-I effects) received positive sigma values (Taft's constants) with the following order: –NO_2 (0.65) > Br (0.44) > -OMe (0.27).[78] Sayiner *et al.*[79] demonstrate that a smaller E_{gap} is generally associated with enhanced antibacterial activity, as it increases the potential for the compounds to interact with bacterial cells and their membranes, ultimately leading to cell death. Essentially, a reduced E_{gap} facilitates easier electron transfer and promotes

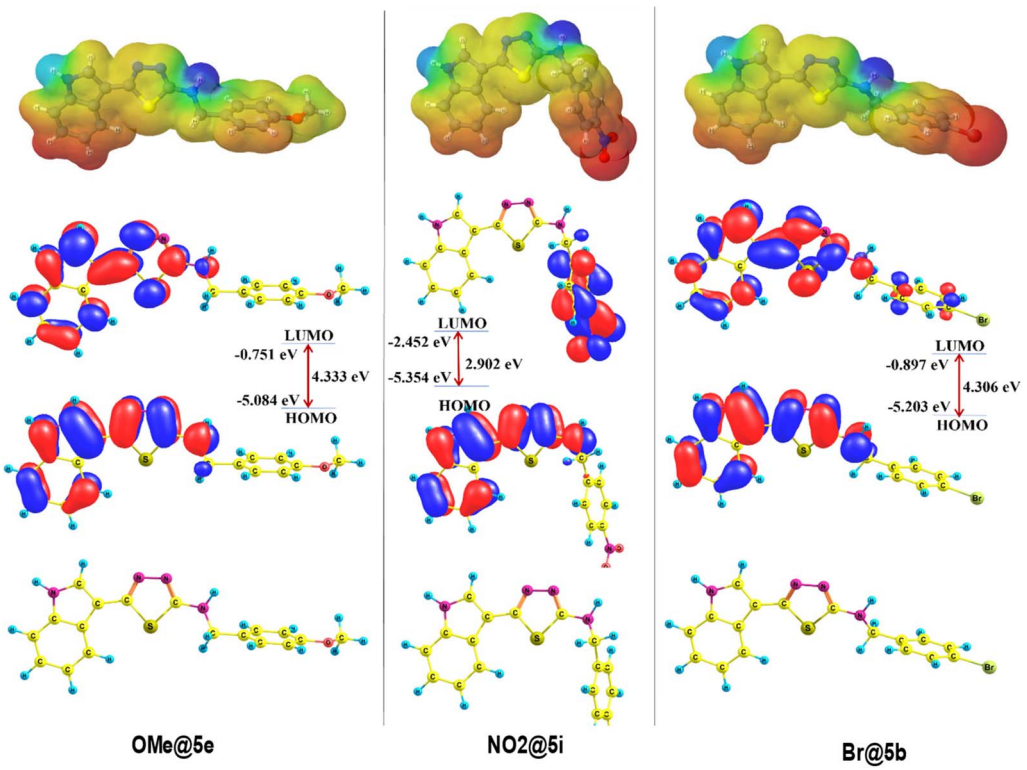

Fig. 2 HOMO–LUMO plots and HOMO–LUMO energy gap values of all three selected molecules.

the generation of harmful radicals. Generally, the trend typically correlates with biological reactivity.[80] Its effect may also depend on the specific biological target involved. The quantum descriptors, including the HOMO–LUMO energy gap ($\Delta E = E_{LUMO} - E_{HOMO}$), absolute electronegativity ($\chi = -(E_{HOMO} + E_{LUMO})/2$), absolute hardness ($\eta = (E_{LUMO} - E_{HOMO})/2$), absolute softness ($\sigma = 1/\eta$), chemical potential ($Pi = -\chi$), and global electrophilicity ($\omega = Pi^2/2\eta$)[79] were calculated, as summarized in Table 3. Dehghanian *et al.*[81] in 2021 reported that a high ω value indicates that a compound is more likely to interact with biological macromolecules, such as proteins and DNA. These results (see Table 3) indicate that the ΔE value for **5i** has the lowest value among the three selected systems, suggesting that **5i** possesses higher chemical reactivity (*i.e.* biologically the most reactive) than the others. In this work, the order of the E_{gap} values for all these three functional group-related compounds is OMe@**5e** (4.333) > Br@**5b** (4.306 eV) > NO_2@**5i** (2.902 eV), which shows that the OMe@**5e** compound is the most stable (chemically least reactive) among all three indolyl-1,3,4-thiadiazol amine-substituted compounds. As described in Table 3, a lower E_{gap} and higher global electrophilicity (ω) value for **5i** indicates its superior reactivity towards the interactions with protein receptors.[82,83] The calculated global electrophilicity (ω) of the investigated compounds showed that compounds **5b** and **5e** featured lower values, indicating comparatively reduced reactivity of the two systems. Overall, the global electrophilicity (ω) values follow the trend **5i** > **5b** > **5e.**

The LUMO value of the –NO_2-related compound shows the most negative value (−2.452 eV) (highest in magnitude), which indicates its most acidic behavior (electron needy). However, the LUMO value of the -OMe group is found to be the lowest negative value (−0.751 eV, lowest in magnitude). Moreover, the HOMOs for both compounds related to -Me and –NO_2 give an opposite trend, as expected. The E_{gap} (2.902 eV) of the NO_2@**5i** compound is the lowest among all the three systems, showing that the NO_2@**5i** system is expected to absorb light with higher wavelengths than the other two compounds with significantly larger E_{gap} values [OMe@**5e** (4.333) > Br@**5b** (4.306 eV)]. The three-dimensional (3D) isosurface maps of the FMOs, such as the HOMOs and LUMOs of all the three selected compounds, are shown in Fig. 2. The HOMOs of all three compounds appeared to be distributed over (in-phase) 5–6 membered fused rings and the next associated 5-membered ring. However, the LUMOs for the OMe@**5e** and Br@**5b** compounds were found to be spread over slightly different (out-phase) on the same rings. Moreover, the LUMOs of the NO_2@**5i** are observed in the NO_2-associated ring. Considering the HOMOs and LUMOs of all three compounds, the electronic transition appears to show from π to π^* transitions.

The electrostatic potential over constant electron density of any chemical species has frequently been acquired by employing the molecular electrostatic potential (MESP) surfaces. The MESP is important owing to its simultaneous display of the local positive and negative potential regions and the sizes and shapes of any chemical species referred to by the color scheme. This is beneficial for exploring the most probable reactive sites (electrophilic and nucleophilic attacks) in relation to the sizes and shapes of molecular systems. The blue (positive), green (neutral), and red (negative) colour regions describe nucleophilic, neutral, and electrophilic attack locations, respectively (see Fig. 2, top). It is observed that the H atom of the N–H group of the bridged C between the two terminal ring segments shows a strong electrophilic nature (electron deficient and electron lover) (shown in dark blue colour, representing the positive region where it can strongly attack the nucleophilic centre). However, the N–H group of the 5-membered ring of the fused ring describes an electrophilic nature but is slightly weaker than the above-mentioned N–H group. Interestingly and importantly, the OMe, NO_2, and Br groups exhibit a nucleophilic nature (electron rich as the nucleus or proton lover) because of the presence of negative charges (shown in red colour, indicating a negative region where an electrophile or proton lover can attack an electrophilic centre) on the O- and Br-atoms.

Table 3 Some calculated electronic parameters (descriptors) using the DFT approach

Entry	Descriptors	5b	5e	5i
1	HOMO (eV)	−5.203	−5.084	−5.354
2	LUMO (eV)	−0.897	−0.751	−2.452
3	E_{gap} (eV)	4.306	4.333	2.902
4	Electronegativity (χ)	3.05	2.917	3.903
5	Absolute hardness (η)	2.153	2.166	1.451
6	Chemical potential (Pi)	−3.05	−2.917	−3.903
7	Absolute softness (σ)	0.464	0.461	0.68
8	Global electrophilicity (ω)	2.16	1.963	5.249

3. Conclusions

We established an iodine-mediated, simple, efficient, and one-pot method for synthesizing indolyl-1,3,4-thiadiazole amine derivatives from indole-3-carboxaldehyde, *p*-toluenesulfonyl hydrazide, and ammonium thiocyanate in a metal-free environment. Furthermore, the synthetic utility of the developed method was achieved by the *N*-functionalization of indolyl-1,3,4-thiadiazole amines using *N*-tosylhydrazones in the presence of CuI and the base. The advantages of our developed protocols include cost-effectiveness; high yield; compatibility with various functional groups, including base-sensitive hydroxy (–OH) functional groups; and no formation of cyanide byproducts. The DFT calculations are utilized to explore the various theoretical aspects and biological properties of the molecules. Among the three chosen systems (**5b**, **5d**, and **5i**), molecule **5i** has the lowest Egap according to DFT analysis, indicating the highest predicted biological activity. Thus, the present work discovers the biological activity of the chosen system, which is theoretically predetermined using DFT. This work opens up opportunities for organic and theoretical chemists to explore further the various biological activities.

Data availability

Data are available in the ESI.†

Conflicts of interest

There are no conflicts to declare.

Acknowledgements

Vartika and M. P. are thankful to Manipal University Jaipur, Department of Chemistry, for providing the lab facilities and infrastructure. The authors would also like to thank the Central Analytical Facilities (CAF) of Manipal University Jaipur for obtaining the IR spectral data.

References

1 F. R. de Sá Alves, E. J. Barreiro and C. A. M. Fraga, *Mini-Rev. Med. Chem.*, 2009, **9**(7), 782–793.
2 M. J. Lai, H. L. Huang, S. L. Pan, Y. M. Liu, C. Y. Peng, H. Y. Lee, T. K. Yeh, P. H. Huang, C. M. Teng, C. S. Chen, H. Y. Chuang and J. P. Liou, *J. Med. Chem.*, 2012, **55**, 3777–3791.
3 D. Davyt, W. Entz, R. Fernandez, R. Mariezcurrena, A. W. Mombrú, J. Saldana, L. Domínguez, J. Coll and E. Manta, *J. Nat. Prod.*, 1998, **61**, 1560–1563.
4 Y. Y. Wang and C. Chen, *J. Chin. Chem. Soc.*, 2007, **54**, 1363–1368.
5 J. Kaur, D. Utreja, N. Jain and S. Sharma, *Curr. Org. Synth.*, 2019, **16**, 17–37.
6 V. Vaishya, R. Singhal, M. K. Mehra and M. Pilania, *ChemistrySelect*, 2023, **8**, e202304377.
7 Z. Zeng, C. Liao and L. Yu, *Chin. Chem. Lett.*, 2024, **35**, 109349.
8 M. Dzurilla, P. Kutschy, J. Zaletova, M. Ruzinsky and V. Kovacik, *Molecules*, 2001, **6**, 716–720.
9 H. Oka, T. Yoshinari, T. Murai, K. Kawamura, F. Satoh, K. Funaishi, A. Okura, H. Suda, M. Okanishi and Y. Shizuri, *J. Antibiot.*, 1991, **44**, 486–491.
10 D. Kumar, S. Sundaree, E. O. Johnson and K. Shah, *Bioorg. Med. Chem. Lett.*, 2009, **19**, 4492–4494.
11 D. Kumar, N. M. Kumar, S. Sundaree, E. O. Johnson and K. Shah, *Eur. J. Med. Chem.*, 2010, **45**, 1244–1249.
12 D. Kumar, N. Maruthi Kumar, K. H. Chang and K. Shah, *Eur. J. Med. Chem.*, 2010, **45**, 4664–4668.
13 D. Kumar, M. K. Narayanam, K.-H. Chang and K. Shah, *Chem. Biol. Drug Des.*, 2011, **77**, 182–188.
14 P. Diana, A. Carbone, P. Barraja, A. Montalbano, A. Martorana, G. Dattolo, O. Gia, L. D. Via and G. Cirrincione, *Bioorg. Med. Chem. Lett.*, 2007, **17**, 2342–2346.
15 B. Bao, Q. Sun, X. Yao, J. Hong, C.-O. Lee, H. Y. Cho and J. H. Jung, *J. Nat. Prod.*, 2007, **70**, 2–8.
16 X. Jing, D. Yuan and L. Yu, *Adv. Synth. Catal.*, 2017, **359**, 1194–1201.
17 I. Kawasaki, M. Yamashita and S. Ohta, *Chem. Pharm. Bull.*, 1996, **44**, 1831–1839.
18 J. Herrmann, A. Abou Fayad and R. Müller, *Nat. Prod. Rep.*, 2017, **34**, 135–160.
19 T. Yi, Q. Liu, Y. Zhang, J. Huang, Z. Zeng and Y. Chen, *Adv. Synth. Catal.*, 2022, **364**, 4097–4102.
20 C. M. Griffiths-Jones and D. W. Knight, *Tetrahedron*, 2011, **67**, 8515–8528.
21 R. González-Lamothe, G. Mitchell, M. Gattuso, M. S. Diarra, F. Malouin and K. Bouarab, *Int. J. Mol. Sci.*, 2009, **10**, 3400–3419.
22 P. Jeandet, *Molecules*, 2015, **20**, 2770–2774.
23 M. S. C. Pedras, M. G. Sarwar, M. Suchy and A. M. Adio, *Phytochemistry*, 2006, **67**, 1503–1509.
24 W. Hu, G. Yan, Q. Ding, J. Cai, Z. Zhang, Z. Zhao, H. Lei and Y. Z. Zhu, *Biomed. Pharmacother.*, 2022, **150**, 112957.
25 S. Schenone, C. Brullo, O. Bruno, F. Bondavalli, A. Ranise, W. Filippelli, B. Rinaldi, A. Capuano and G. Falcone, *Bioorg. med. chem.*, 2006, **14**, 1698–1705.
26 F. Clerici, D. Pocar, M. Guido, A. Loche, V. Perlini and M. Brufani, *J. Med. Chem.*, 2001, **44**, 931–936.
27 S. Turner, M. Myers, B. Gadie, S. A. Hale, A. Horsley, A. J. Nelson, R. Pape, J. F. Saville, J. C. Doxey and T. L. Berridge, *J. Med. Chem.*, 1988, **31**, 906–913.
28 L. Labanauskas, V. Kalcas, E. Udrenaite, P. Gaidelis, A. Brukstus and V. Dauksas, *Die Pharmazie*, 2001, **56**, 617–619.
29 B. Sharma, A. Verma, S. Prajapati and U. K. Sharma, *Int. J. Med. Chem.*, 2013, **2013**, 348948.
30 G. Mazzone, R. Pignatello, S. Mazzone, A. Panico, G. Pennisi, R. Castana and P. Mazzone, *Farmaco*, 1993, **48**, 1207–1224.
31 U. F. Mansoor, A. R. Angeles, C. Dai, L. Yang, D. Vitharana, A. D. Basso, K. Gray, H. Tang, M. Liu and L. Liang, *Bioorg. med. chem.*, 2015, **23**, 2424–2434.
32 S. K. Mohanty, N. Y. Subbaiah, M. V. Madhavi, K. Manda, K. Raju, E. Jajili, D. N. L. Divya and B. N. Sudha, *J. Pharm. Negat. Results*, 2022, 4685–4691.
33 A. R. Bhat, Tazeem, A. Azam, I. Choi and F. Athar, *Eur. J. Med. Chem.*, 2011, **46**, 3158–3166.
34 E. E. Oruç, S. Rollas, F. Kandemirli, N. Shvets and A. S. Dimoglo, *J. Med. Chem.*, 2004, **47**, 6760–6767.
35 L. Bonina, D. Iannello, R. Merendino, A. Arena and P. Mastroeni, *Infect. Immun.*, 1983, **39**, 575–579.
36 G. Akalin Çiftçi, B. Sever and M. D. Altintop, *Turk. J. Pharm. Sci.*, 2019, **16**, 119–131.
37 X. Ma, L. Yu, C. Su, Y. Yang, H. Li and Q. Xu, *Adv. Synth. Catal.*, 2017, **359**, 1649–1655.
38 E. C. Pham, T. N. Truong, N. H. Dong, D. D. Vo and T. T. Hong Do, *Med. Chem.*, 2022, **18**, 558–573.
39 D. Kumar, N. M. Kumar, B. Noel and K. Shah, *Eur. J. Med. Chem.*, 2012, **55**, 432–438.
40 T. Liu, Y. Wan, R. Liu, L. Ma, M. Li and H. Fang, *Chem. Res. Chin. Univ.*, 2016, **32**, 768–774.
41 P. Taya, D. K. Mehta and R. Das, *Int. J. Pharm. Sci. Res.*, 2019, **10**, 701–711.
42 S. Cascioferro, B. Parrino, G. L. Petri, M. G. Cusimano, D. Schillaci, V. Di Sarno, S. Musella, E. Giovannetti, G. Cirrincione and P. Diana, *Eur. J. Med. Chem.*, 2019, **167**, 200–210.
43 N. Perike, P. K. Edigi, N. Gurrapu, S. D. Nagulapally, S. Bujji and N. J. P. Subhashini, *Asian J. Chem.*, 2024, **36**, 1946–1952.
44 Akanksha, A. K. Singh, A. Asthana, R. Ravi and A. Kishor Jha, *Asian J. Org. Chem.*, 2024, **13**, e202400232.

45 J. Barluenga and C. Valdés, *Mod. Heterocycl. Chem.*, 2011, 377–531.
46 V. Vaishya, R. Singhal, T. Kriplani and M. Pilania, *Synthesis*, 2022, **54**, 3941–3961.
47 R. Singhal, S. P. Choudhary, B. Malik and M. Pilania, *ChemistrySelect*, 2022, **7**, e202200134.
48 X. Zhang, P. Sivaguru, Y. Pan, N. Wang, W. Zhang and X. Bi, *Chem. Rev.*, 2025, **125**, 1049–1190.
49 E. E. Oruç, S. Rollas, F. Kandemirli, N. Shvets and A. S. Dimoglo, *J. Med. Chem.*, 2004, **47**, 6760–6767.
50 J. K. Mahadev, C. A. Nandkumar, K. A. Vishveswar, S. PL and P. VJ, *Asian J. Pharm. Res. Dev.*, 2024, **12**, 129–143.
51 M. Padmapriya, S. S. Hakkimane and S. L. Gaonkar, *Discover Appl. Sci.*, 2025, **7**, 1–53.
52 S. Ahmad, M. Z. Alam, U. Salma, M. Mohasin, P. F. Rahaman, H. Parveen and S. A. Khan, *J. Mol. Struct.*, 2024, 138438.
53 V. Bhaskar, P. Mohite and J. Optoelectron, *Biomed. Mater*, 2010, **2**, 249–259.
54 A. Ansari, A. Ali and M. Asif, *New J. Chem.*, 2017, **41**, 16–41.
55 S. Ananthula, P. Parajuli, F. A. Behery, A. Y. Alayoubi, K. A. El Sayed, S. Nazzal and P. W. Sylvester, *Anticancer res.*, 2014, **34**, 2715–2726.
56 A. Monga, S. Bagchi and A. Sharma, *New J. Chem.*, 2018, **42**, 1551–1576.
57 J.-Q. Wang, Z.-Y. Zuo and W. He, *Catalysts*, 2022, **12**, 821.
58 R. Singhal, S. P. Choudhary, B. Malik and M. Pilania, *RSC Adv.*, 2024, **14**, 5817–5845.
59 S. S. Acharya, S. Patra, L. M. Barad, A. Roul and B. B. Parida, *New J. Chem.*, 2024, **48**, 7614–7638.
60 D. R. Guda, H. M. Cho and M. E. Lee, *RSC Adv.*, 2013, **3**, 7684–7687.
61 W. Yu, G. Huang, Y. Zhang, H. Liu, L. Dong, X. Yu, Y. Li and J. Chang, *J. Org. Chem.*, 2013, **78**, 10337–10343.
62 P. Niu, J. Kang, X. Tian, L. Song, H. Liu, J. Wu, W. Yu and J. Chang, *J. Org. Chem.*, 2015, **80**, 1018–1024.
63 M. T. Javid, F. Rahim, M. Taha, H. U. Rehman, M. Nawaz, S. Imran, I. Uddin, A. Mosaddik and K. M. Khan, *Bioorg. chem.*, 2018, **78**, 201–209.
64 P. Finkbeiner and B. J. Nachtsheim, *Synthesis*, 2013, 979–999.
65 Y.-M. Ren, C. Cai and R.-C. Yang, *RSC Adv.*, 2013, **3**, 7182–7204.
66 H. Togo and S. Iida, *Synlett*, 2006, **2006**, 2159–2175.
67 G. R. Reddy, T. R. Reddy, S. C. Joseph, K. S. Reddy and M. Pal, *RSC Adv.*, 2012, **2**, 3387–3395.
68 J. Yadav, B. S. Reddy, K. Premalatha and T. Swamy, *Tetrahedron Lett.*, 2005, **46**, 2687–2690.
69 N. Mulakayala, P. Murthy, D. Rambabu, M. Aeluri, R. Adepu, G. Krishna, C. M. Reddy, K. Prasad, M. Chaitanya and C. S. Kumar, *Bioorg. Med. Chem. Lett.*, 2012, **22**, 2186–2191.
70 F. Zhu, Z. Yan, C. Ai, Y. Wang and S. Lin, *Eur. J. Org Chem.*, 2019, **2019**, 6561–6565.
71 M. Pilania, A. Velladurai, M. P. Tantak and D. Kumar, *ChemistrySelect*, 2016, **1**, 6368–6373.
72 C. Lei, Y. J. Yip and J. S. Zhou, *J. Am. Chem. Soc.*, 2017, **139**, 6086–6089.
73 Y. Lu, Y. Sun, A. Abdukader and C. Liu, *Synlett*, 2021, **32**, 1044–1048.
74 M. Frisch, G. Trucks, H. Schlegel, G. Scuseria, M. Robb, J. Cheeseman, G. Scalmani, V. Barone, B. Mennucci and G. Petersson, in *Gaussian 09*, Gaussian Inc Wallingford, 2009.
75 S. K. Pandey, *ACS omega*, 2021, **6**, 31077–31092.
76 S. K. Pandey, *ACS omega*, 2021, **6**, 11711–11728.
77 S. Awasthi, J. K. Gaur, S. K. Pandey, M. S. Bobji and C. Srivastava, *ACS Appl. Mater. Interfaces*, 2021, **13**, 24505–24523.
78 R. W. Taft Jr and I. C. Lewis, *J. Am. Chem. Soc.*, 1958, **80**, 2436–2443.
79 M. Feizi-Dehnayebi, E. Dehghanian and H. Mansouri-Torshizi, *Spectrochim. Acta, Part A*, 2021, **249**, 119215.
80 P. Sharma, R. Prabhat and T. Chakraborty, *Mol. Phys.*, 2024, **122**, e2331620.
81 M. Feizi-Dehnayebi, E. Dehghanian and H. Mansouri-Torshizi, *J. Mol. Struct.*, 2021, **1240**, 130535.
82 M. Er, B. Ergüven, H. Tahtaci, A. Onaran, T. Karakurt and A. Ece, *Med. Chem. Res.*, 2017, **26**, 615–630.
83 M. Er, A. Özer, Ş. Direkel, T. Karakurt and H. Tahtaci, *J. Mol. Struct.*, 2019, **1194**, 284–296.